HIROSAKI UNIVERSITY

Radiation Environment and Medicine 2023 Vol.12, No.1 65–73

REM
Radiat Environ Med

Regular Article

Effect of Ionizing Radiation on the Intercellular Network of Murine Cerebral Cortical Neurons

Masaru Yamaguchi[1§], Takakiyo Tsujiguchi[1§], Tomonori Furukawa[2], Shuji Shimoyama[2], Toshiya Nakamura[3], Yasushi Mariya[4] and Junko Yamada[5*]

[1]*Department of Radiation Science, Hirosaki University Graduate School of Health Sciences, 66-1 Hon-cho, Hirosaki, Aomori 036-8564, Japan*
[2]*Department of Neurophysiology, Hirosaki University Graduate School of Medicine, 5 Zaifu-cho, Hirosaki, Aomori 036-8562, Japan*
[3]*Department of Bioscience and Laboratory Medicine, Hirosaki University Graduate School of Health Sciences, 66-1 Hon-cho, Hirosaki, Aomori 036-8564, Japan*
[4]*Aomori Rosai Hospital, 1 Shirogane-machi, Hachinohe, Aomori 031-8551, Japan*
[5]*Department of Comprehensive Rehabilitation Science, Hirosaki University Graduate School of Health Sciences, 66-1 Hon-cho, Hirosaki, Aomori 036-8564, Japan*

Received 13 September 2022; revised 25 November 2022; accepted 7 December 2022

Depending on brain tumor type, radiotherapy with various irradiation methods may be an effective treatment even for lesions for which surgical treatment is difficult; however, neurocognitive dysfunction may occur as an adverse effect. Neurons divide infrequently and are recognized as radiation resistant; however, few reports have investigated the effects of radiation on the intercellular network. We analyzed the impact of radiation exposure on the repair kinetics of DNA damage and the electrophysiological changes of synaptic currents in cerebral cortical neurons, employing primary culture technique. Cortical neurons (14 days *in vitro*) were subjected to varying X-irradiation doses. DNA double-strand breaks were induced in cultured cortical neurons by high-dose X-irradiation; however, these cells have the ability to repair severe DNA damage and are resistant to radiation. An electrophysiological investigation revealed that the inter-event intervals of miniature excitatory postsynaptic current (mEPSC) in X-irradiated cortical neurons were significantly longer, while the amplitude showed no change in comparison to 0 Gy-irradiated cells. These results suggested that the exposure of neurons to radiation led to a decrease in the frequency of the mEPSC, which affected the synaptic network, which supports the neurocognitive function despite being less likely to cause cell death or severe DNA damage.

Key words: ionizing radiation, cerebral cortical neurons, electrophysiology, postsynaptic current

1. Introduction

Malignant neoplasms are the leading cause of death in Japan, accounting for 30% of all deaths[1)]. Radiotherapy is a topical treatment for cancer. It is considered less invasive and capable of preserving the function and morphology of organs. Radiotherapy is widely used to treat malignant tumors (e.g., primary and metastatic brain tumors and head/neck cancers) and improves the

*Junko Yamada: Department of Comprehensive Rehabilitation Science Hirosaki University Graduate School of Health Sciences 66-1 Hon-cho, Hirosaki, Aomori 036-8564, Japan
E-mail: jyamada@hirosaki-u.ac.jp
[§]These authors have made an equivalent contribution to the first author.
https://doi.org/10.51083/radiatenvironmed.12.1_65

prognosis of these patients[2-4]; however, radiotherapy may unavoidably induce injury to the healthy central nervous system (CNS) surrounding the tumor[5-9]. Cerebral necrosis, leukoencephalopathy, and cerebral atrophy are well known examples of radiation-induced damage to the CNS[10-17]. Although classic radiation necrosis has become less common, it is increasingly reported that subtle CNS toxicities (e.g., progressive cognitive dysfunction or impairment of the neurocognitive function (NCF)) may occur within the classically "tolerable" radiation dose range of approximately 20–30 Gy in 10 fractions within 3 weeks[8, 18-22]. On the other hand, Mariya *et al.* reported that neurofunctional recovery was observed in a large proportion of patients who received radiotherapy for brain tumors[23]. In addition, Aoyama *et al.* demonstrated that whole brain radiotherapy affected the NCF of patients with brain metastases who received stereotactic radiosurgery, and that brain tumor control is the most important factor for stabilizing the NCF; however, the long-term adverse effects of whole brain radiotherapy on the NCF might not be negligible[19]. The presence of restoration or stabilization of the CNS function may reflect plasticity of the residual neurons and their networks against CNS damage caused by the tumor itself and radiation exposure[24]; however, this remains to be clarified. Although neurons are generally thought to be resistant to radiation[25], there is a scarcity of detailed information regarding how radiation affects neurons and synaptic transmission and causes memory impairment. Hence, to elucidate the genetic damage/repair and electrophysiological changes in synaptic transmission that could underlie the neuroplasticity, we investigated the impact of radiation exposure on the repair kinetics of DNA double-strand breaks (DSBs) and serial changes of synaptic currents in cerebral cortical neurons, employing primary culture.

2. Materials and methods

2.1. Ethics statement

All experiments were conducted according to the legal regulations in Japan and the Guidelines for Animal Experiments after obtaining approval from the animal experimental committee (approved number: G140006), and all efforts were made to minimize the number of animals used and their suffering in this study. All mice were housed in standard cages in a conventional clean room under a 12-h light/dark cycle. The mice had *ad libitum* access to sterilized standard laboratory mouse chow diet and drinking water.

2.2. Primary cultures of embryonic mouse cerebral cortical neurons

Primary neuronal cortical cultures were prepared as described previously[26]. Briefly, cerebral cortices were dissected from C57BL/6JJcl mice (Clea Japan, Tokyo, Japan) embryos at 15–16 days of gestation (8–10 embryos from 13 dams each). After removal of the meninges, the cortices were cut into small pieces (< 1 mm^3) in phosphate-buffered saline (PBS). The tissue was sedimented and washed three times with Dulbecco's modified Eagle's medium (Invitrogen, Carlsbad, CA, USA), and then incubated at 37 ℃ for 10 min in an enzyme solution containing 2.5 mg/mL trypsin and 0.01% DNase I (Sigma-Aldrich, St. Louis, MO, USA). After enzymatic digestion and mechanical trituration in serum-free medium, the cells so obtained were suspended in the medium. Cells were plated on poly-L-lysine-coated coverslips in 24-well culture plates at 2.0 $\times 10^5$ cells in 1 mL/well, and maintained in serum-free medium. The serum-free culture medium consisted of Neurobasal medium (Invitrogen) supplemented with 2% B27 supplement (Invitrogen), 0.5 mM L-glutamine, and 100 units/mL penicillin-streptomycin (Invitrogen). Half of the volume of the medium was replenished twice a week. Cells were cultured under these conditions for 14 days *in vitro* (DIV14 cortical neurons) and used for the following irradiation experiments. The number of viable cells was counted on day 7 using the trypan blue dye exclusion method (Sigma-Aldrich) after collected cortical neurons with 0.1% trypsin-ethylene diamine tetraacetic acid (Gibco; Thermo Fisher Scientific).

2.3. In vitro irradiation with X-rays

DIV14 cortical neurons in serum-free medium were subjected to varying X-irradiation doses of 0, 0.1, 0.5, 1, 2, 4 or 7 Gy (150 kVp, 20 mA, 0.5-mm aluminum and 0.3-mm copper filters) at a dose rate of 1.0 Gy/min using an MBR-1520R X-ray generator (Hitachi Medical, Tokyo, Japan) at a distance of 45 cm between the focus and the target. The dose was monitored with a thimble ionization chamber that was placed next to the sample during irradiation and dishes containing DIV14 cortical neurons were arranged concentrically.

2.4. Measurement of cell death

For detection of cell death, the cells were first washed twice with cold PBS and then fixed with 4% paraformaldehyde for 30 min. The fixed cells were washed again with PBS and mounted using Vectashield® Mounting Medium with 4',6-diamidino-2-phenylindole (DAPI, Vector Laboratories, Burlingame, CA, USA). The cell death was examined under an Olympus IX71 fluorescent microscope (Tokyo, Japan) and its DP2-BSWsoftware with a magnification of 40. Cells containing condensed nuclei were considered to be dead. Data were collected from at least three random sections per dish.

2.5. Immunofluorescent detection of DNA DSB repair related proteins

DIV14 cortical neurons were washed with PBS, and fixed with ice-cold 75% ethanol for 10 min at room temperature. Fixed cells were washed with PBS, permeabilized in 0.5% Triton X-100 (Wako, Osaka, Japan) on ice for 5 min, and washed twice with PBS. The cells were then incubated with an anti-phospho-histone H2AX (ser139) mouse immunoglobulin G monoclonal antibody and anti-53BP1 mouse immunoglobulin M monoclonal antibody (Millipore, Billerica, MA, USA) diluted 1:300-fold with TBST (20 mM Tris-HCl [pH 7.4], 137 mM NaCl, 0.1% TWEEN-20) containing 5% skim milk at 37 ℃ for 120 min, and subsequently washed with PBS and incubated with Alexa Fluor 488 goat anti-mouse immunoglobulin G (H+L) antibody and Alexa Fluor 546 goat anti-mouse immunoglobulin M (μ chain) antibody diluted 1:400-fold with TBST containing 5% skim milk at 37 ℃ for 60 min. Following a second wash with PBS, the cells were adhered to microscope glass slides (Matsunami Glass, Osaka, Japan) using a StatSpin® CytoFuge 2 (Iris Sample Processing, Westwood, MA, USA) and mounted using Vectashield® Mounting Medium with DAPI. For the quantitative analysis, the phosphorylation of the histone variant H2AX at serine 139 (γ-H2AX) and tumour suppressor p53 binding protein1 (53BP1) foci were counted per cell using a Laser Scanning Microscope 710 (Carl Zeiss Microscopy, Tokyo, Japan) with a magnification of 63[27, 28]. Under blinded conditions, the numbers of γ-H2AX and 53BP1 foci per cell were counted for more than 50 cells in every sample.

2.6. Electrophysiology

As we reported in previous papers[26, 29], the synaptic currents were measured by voltage-clamp and patch-clamp method to analyse changes in neuronal transmission. DIV14 cortical neurons were transferred to a recording chamber on the stage of an upright microscope ECLIPSE E600FN (Nikon, Tokyo, Japan), continuously perfused with artificial cerebrospinal fluid (ACSF) at a flow rate of 1−2 mL/min at 31−32 ℃, and viewed on a monitor with infrared differential interference contrast. The standard ACSF contained 126 mM sodium chloride, 2.5 mM potassium chloride, 1.25 mM sodium dihydrogen phosphate, 2.0 mM magnesium sulfate, 2.0 mM calcium chloride, 26.0 mM sodium bicarbonate and 20.0 mM glucose with 95% O_2 and 5% CO_2. The resting membrane potential and membrane resistance were recorded before miniature excitatory postsynaptic current (mEPSC) without tetrodotoxin (TTX). mEPSC recordings were obtained in whole cell voltage-clamp mode with holding potential at -70 mV in the presence of 1 μM tetrodotoxin. Patch electrodes had 4−5 MΩ resistance when filled with a solution containing 150 mM potassium methane sulfonate, 5 mM potassium chloride, 0.5 mM ethylene glycol-bis (2-aminoethylether)-N,N,N',N'-tetra acetic acid, 10 mM 4-(2-hydroxyethyl)-1-piperazineethanesulfonic acid, 3 mM magnesium (adenosine triphosphate)$_2$, and 0.4 mM guanosine triphosphate; pH 7.3. Patch electrodes were fabricated from borosilicate capillary tubing of 1.5 mm in diameter (Garner Glass, Claremont, CA, USA) using a Narishige PP-83 vertical puller (Narishige, Tokyo, Japan). Recordings were made with a MultiClamp 700B amplifier (Molecular Devices, CA, USA) in conjunction with a Digidata 1322A digitizer (Molecular Devices) and the pClamp 10 software suite for the Clampex software (Molecular Devices). All signals were filtered at 2 kHz and sampled at 10 kHz. mEPSCs were recorded at least 3 min. Averaged values of all cells were showed in every 30 s for amplitude and inter-event intervals of mEPSCs analyzed using the Mini Analysis program (Synapto soft, USA) with a threshold of 6 pA for event detection.

2.7. Statistical analyses

Significance levels were calculated using the Origin software package (Origin Lab, Northampton, MA, USA) for the Windows operating system. The *t* test was used for the comparisons between two groups, while the Steel test was used for the comparisons among multiple groups. *P* values of 0.05 were considered to indicate statistically significant differences.

3. Results

3.1. Cell viability and repair kinetics of DNA DSB in murine cerebral cortical neurons

In order to investigate the response of DIV14 cortical neurons to high dose of X-rays in this study, the number of viable cells was counted one week later using the trypan blue dye exclusion method and DAPI nuclear staining. As shown in Fig. 1A, almost cortical neurons subjected to X-irradiation doses of 0 Gy (left panel) or 7 Gy (right panel) were not shrunken. Cortical neurons retained the ability to grow after exposure to 7 Gy, and no statistically significant differences in viable cell numbers were observed between non-irradiated and 7 Gy-irradiated cells (P = 0.6176, Fig. 1B). Additionally, we next compared X-irradiation-induced cell death (Fig. 1C). DAPI nuclear staining observed by fluorescence microscopy showed normal nuclear labeling as very diffuse large intact structures, rather than bright small bodies which is a typical feature of nuclear condensation. The number of apoptotic cells labeled by DAPI did not appear to increase after X-irradiation, relative to control. No significant effects on cell viability were detected between non-irradiated (75.6 ± 9.4%) and 7 Gy-irradiated cells (72.3 ± 5.4%, P = 0.3140, Fig. 1D). These data indicate that the cytotoxicity of X-rays was not severe in immature

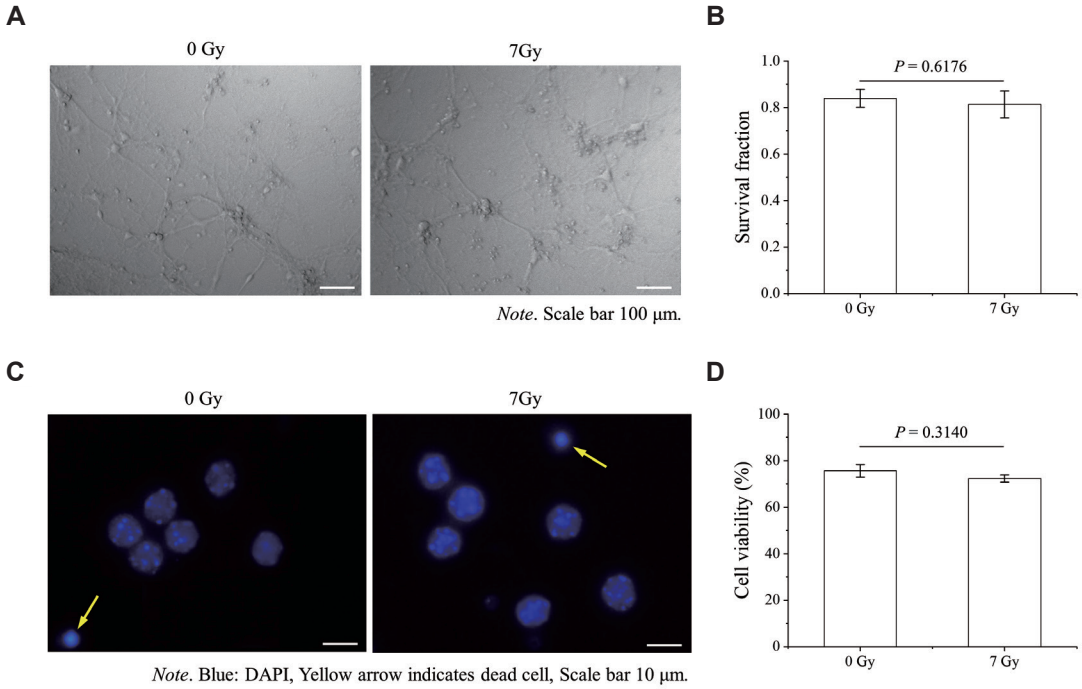

Fig. 1. Cell viability assessment of X-irradiated DIV14 cortical neurons. [A] Representative photographs of cultured cortical neurons at one week after X-irradiation are shown in the left (0 Gy) and right panel (7 Gy) (10×magnifications, scale bar 100 μm). [B] Viable cells in each condition were counted using the trypan blue dye exclusion method and the surviving fraction was calculated based on initial number of seeded cells (2.0×10^5 cells/ml). The data are expressed as the mean±standard deviation (SD) of 3 independent experiments. [C] Representative photomicrographs of DAPI-stained nuclei of cortical neurons are shown in the left (0 Gy) and right panel (7 Gy) (40×magnifications, scale bar 10 μm). Yellow arrow indicates radiation-induced nuclear condensation considered to be dead. [D] Cell viability relative to total cell count in at least three random sections per dish (n = 12 in each condition). The data are expressed as the mean ± standard error (SE). No statistically significant differences were observed between two groups by t test.

neurons. In order to evaluate the DNA DSB formation and repair kinetics of DIV14 cortical neurons, the foci of γ-H2AX, a DNA DSB marker, and the DNA damage response protein 53BP1, which interacts with γ-H2AX to co-localize to the DSB site and accurately repair DNA damage, were analyzed in these cells subjected to varying X-irradiation doses of 0, 0.1, 0.5, 1, 2, or 4 Gy and harvested from 0.5 h to 168 h post-irradiation, and a representative image is shown in Figure 2A. A radiation-dose dependent increase in the numbers of γ-H2AX and 53BP1 foci after X-irradiation was observed in cortical neurons. In 0.1−4 Gy-irradiated cells, the number of γ-H2AX foci peaked at 0.5−1 h after X-irradiation, and was approximately 10−68 fold higher than that in non-irradiated cells (Fig. 2B, Table 1). Similar to the results observed in the γ-H2AX expression, the number of 53BP1 foci of 0.1−4 Gy-irradiated cortical neurons was approximately 10−60 fold higher than that of non-irradiated cells at 0.5−1 h after X-irradiation (Fig. 2C, Table 1). Although the γ-H2AX and 53BP1 foci per nucleus of the irradiated cells began to gradually decrease after 1 h, the numbers of residual foci of γ-H2AX and 53BP1 in the 2−4 Gy-irradiated cortical neurons were still significantly higher (2−15 fold and 6−14 fold, respectively) in comparison to non-irradiated cells at 12 and 24 h after X-irradiation. After 48 h have passed, the numbers of γ-H2AX and 53BP1 foci decreased to the same level as in non-irradiated cells. These results suggested that DNA DSB were induced in cultured DIV14 cortical neurons by X-irradiation; however, these cells have the ability to repair severe DNA damage and are resistant to radiation.

3.2. Effect of X-irradiation exposure on the synaptic responses of murine cerebral cortical neurons

First, we observed the membrane property of each group. Before applied TTX, cortical neurons were recorded the resting membrane potential and resistance by current clamp mode. There were no significant differences in all groups (Fig. 3A and 3B). Neurons and their synapses are the basic building blocks of a complex giant network of the brain, and transmitted information is coded by the timing and number of action potentials, which is generated by the opening of voltage-gated sodium channels during depolarization. For analyzing of the effect of irradiation on the synapse, we used mEPSCs, which indicates the single quantum synaptic responses[30]. These mEPSCs can be detected during total blockade of action potentials by TTX. In order to clarify the effects of

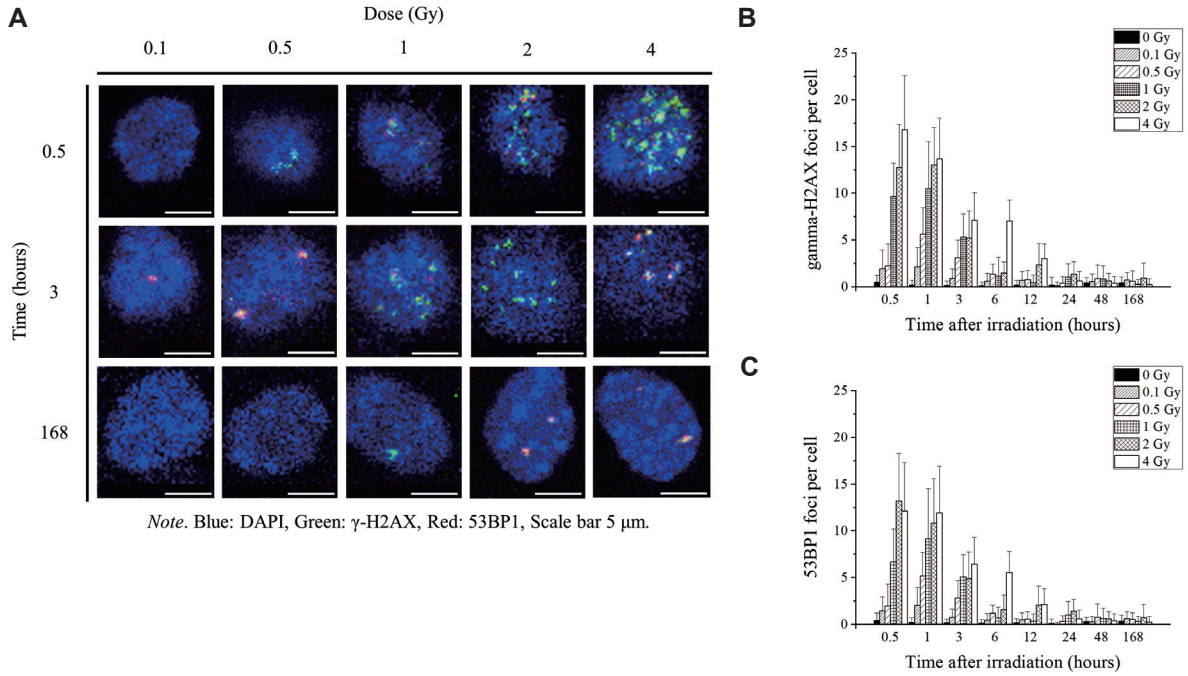

Note. Blue: DAPI, Green: γ-H2AX, Red: 53BP1, Scale bar 5 μm.

Fig. 2. DNA DSB formation and repair kinetics. [A] Representative co-localized images of γ-H2AX and 53BP1 in cortical neurons obtained 0.5 h, 3 h, and 168 h after X-irradiation with 0.1 − 4 Gy. Nuclei, γ-H2AX foci, and 53BP1 foci are shown in blue, green, and red, respectively (63× magnifications, scale bar 5 μm). [B] γ-H2AX and [C] 53BP1 foci were counted in each cell. Data are expressed as the mean ± SD of 3 independent experiments for each dose and time point. A Steel multiple comparison test revealed statistically significant differences among cells irradiated with 0 Gy to 4 Gy of X-rays and statistical details were summarized in Table 1.

Table 1. Summary of fold-change (FC) with *P* value in DNA double-strand break repair kinetics.

hrs \ Gy		γ-H2AX foci number normalized by 0 Gy					53BP1 foci number normalized by 0 Gy				
		0.1 Gy	0.5 Gy	1 Gy	2 Gy	4 Gy	0.1 Gy	0.5 Gy	1 Gy	2 Gy	4 Gy
0.5 h	FC	4.0	4.7	20.2	26.5	35.0	3.4	4.7	15.9	31.4	28.9
	P value	0.0370	0.0111	< .0001	< .0001	< .0001	-	0.0154	< .0001	< .0001	< .0001
1 h	FC	10.7	28.1	52.4	65.1	68.3	10.1	25.9	45.8	54.3	59.6
	P value	-	< .0001	< .0001	< .0001	< .0001	0.0148	< .0001	< .0001	< .0001	< .0001
3 h	FC	5.1	17.2	29.6	28.9	39.6	4.8	17.6	31.6	30.5	40.3
	P value	-	< .0001	< .0001	< .0001	< .0001	-	< .0001	< .0001	< .0001	< .0001
6 h	FC	4.1	9.7	8.3	10.4	50.3	3.3	8.4	4.9	11.3	39.7
	P value	-	< .0001	0.0002	< .0001	< .0001	-	0.0001	0.0450	< .0001	< .0001
12 h	FC	3.5	3.9	2.1	11.8	15.2	2.8	3.1	1.9	11.6	12.0
	P value	-	-	-	< .0001	< .0001	-	-	-	< .0001	< .0001
24 h	FC	0.5	1.7	4.7	6.3	2.8	0.4	3.0	10.0	14.0	6.0
	P value	-	-	< .0001	< .0001	0.0002	-	-	0.0009	0.0104	0.0104
48 h	FC	1.3	2.1	2.0	1.5	0.9	0.9	2.6	2.1	1.9	1.3
	P value	-	-	-	-	-	-	-	-	-	-
168 h	FC	1.7	1.4	0.7	2.2	0.6	1.8	1.4	0.8	2.0	0.7
	P value	-	-	-	-	-	-	-	-	-	-

Note. FC shows that the average foci number of γ-H2AX or 53BP1 at each dose is normalized by that of the 0 Gy. No value " - " means there was no statistically significant difference ($P > 0.05$). *P* values of 10^{-5} or less were unified as "< .0001".

X-ray exposure on the glutamatergic excitatory synapses, representative images of DIV14 cortical neurons were taken 2 − 3 days after X-irradiation with 0 Gy, 2 Gy, 4 Gy, and 7 Gy using whole-cell patch-clamp recordings. The mEPSC waveforms are shown below each representative image, and the vertical and horizontal directions of the waveform indicate the amplitude and the frequency, respectively (Fig. 3C). The amplitude reflects the sensitivity to transmitters in the postsynaptic membranes and the frequency (inter-event intervals) reflects the probability of transmitter release from the synaptic terminal. Although no significant effects on the amplitude of mEPSC were observed in cortical neurons subjected to X-irradiation doses of up to 7 Gy (Fig. 3D), the inter-event intervals of mEPSC in 4 Gy-irradiated cortical neurons (235.2 ± 42.3 msec, $P = 0.0093$) and 7 Gy-irradiated cortical

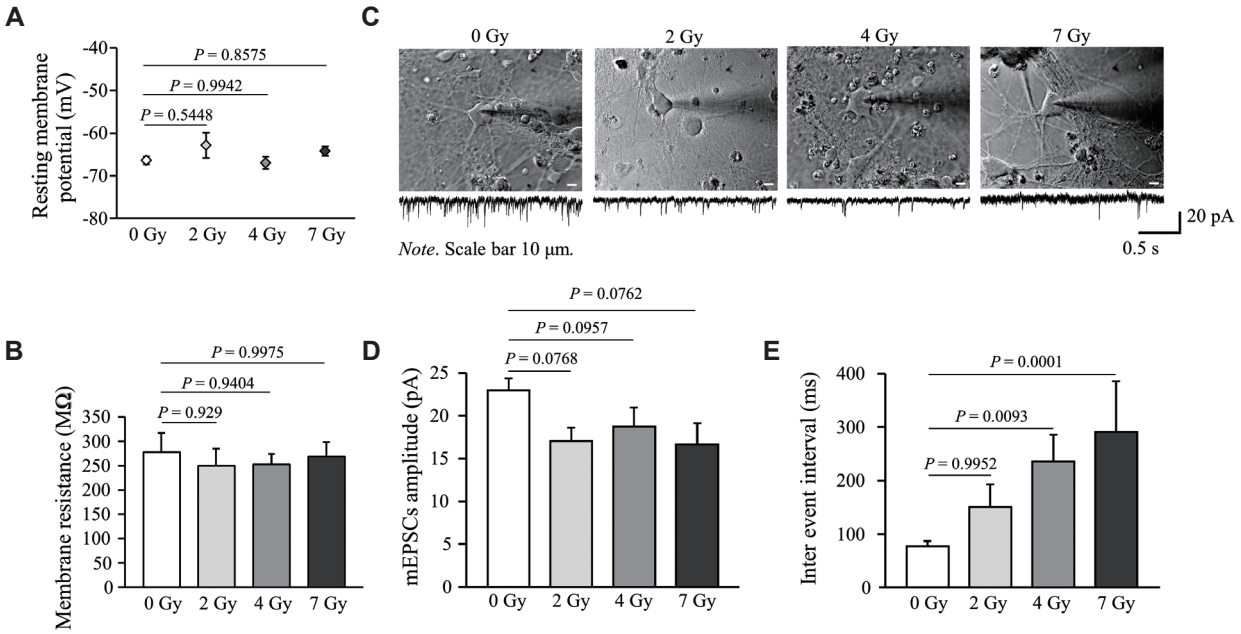

Fig. 3. Membrane properties and alterations in mEPSC. [A] The mean resting membrane potential and [B] membrane resistance measured by current injection in 0 – 7 Gy (n = 6 ~ 8 each). [C] Representative images and recordings of cortical neurons taken 2 – 3 days after X-irradiation with 0 – 7 Gy. Scale bar, 10 μm. The mEPSC tracing is shown below the cell image. The effect of X-irradiation on [D] mEPSC amplitude (pA) and [E] inter-event interval (msec). Error bars represent the mean ± SE in 0 Gy (n = 31, 16 plates), 2 Gy (n = 16, 8 plates), 4 Gy (n = 19, 10 plates), and 7 Gy (n = 15, 8 plates) irradiated groups, respectively. The statistical significance of differences among 0 Gy-, 2 Gy-, 4 Gy-, and 7 Gy-irradiated groups was evaluated by the Steel multiple comparison test.

neurons (291.5 ± 94.5 msec, P = 0.0001) were significantly longer in comparison to non-irradiated cells (77.8 ± 9.0 msec) (Fig. 3E), suggesting that radiation exposure reduces the frequency of the mEPSC and causes a decrease in the release of transmitters from the synaptic terminal.

4. Discussion

The aim of this study was to investigate the effect of radiation exposure on the repair kinetics of DNA DSB and the serial changes in the synaptic network in embryonic murine cerebral cortical neurons, employing a primary culture technique. This useful technique has already been reported in several papers in order to elucidate the neurotoxic action of organotin compounds and to clarify the activation mechanism of K^+Cl^- co-transporter function by brain-type creatinine kinase, suggesting that an *in vitro* model of dissociated cortical neurons recapitulates the connectivity within the intact cortex[26, 31]. Furthermore, morphological and electrophysiological changes in intratelencephalic-type pyramidal neurons in the motor cortex of a rat model of levodopa-induced dyskinesia were investigated, which shows how abnormal transmission between synapses impairs central nervous system function[29]. Neural stem cells and vascular endothelial cells are generally radioresistant; however, these cellular disorders cause the suppression of neurogenesis, a progressive reduction in the survival of clonogenic cells, ischemic changes, and the break-down of the blood brain barrier, which causes regression and the deterioration of the neuronal network and function[8, 32-35]. For both patients undergone radiation for brain tumors and their caregivers, the distressing adverse effect is impaired cognition. This debilitating effect have suffered from inadequate understanding of the cellular mechanisms of radiation damage, and little information exists on the acute effects of radiation on synaptic function. In this study, after 48 h passed, DNA DSB formation, which was monitored by immunocytochemistry of γ-H2AX and 53BP1, returned to the baseline levels of non-irradiated cells, and the cortical neurons used in this study were found to have the ability to repair severe DNA damage and to be resistant to high-dose irradiation (Fig. 1 and Fig. 2). On the other hand, no significant effects on the amplitude of mEPSC, sensitivity to transmitters in the postsynaptic membranes, was observed in cortical neurons subjected to X-irradiation doses of up to 7 Gy (Fig. 3D). However, the inter-event intervals of mEPSC, reflecting the probability of transmitter release from the synaptic terminal, in 4 Gy and 7 Gy-irradiated cortical neurons were significantly longer in comparison to non-irradiated cells (Fig. 3E). Radiation exposure reduces the frequency of mEPSC; thus, decreasing the release of transmitters from the

synaptic terminal. However, the lack of a significant effect on the amplitude of mEPSC implies that the susceptibility of transmitter receptors at the postsynapse was unaffected by radiation exposure. In other words, radiation exposure presynaptically suppressed the synaptic transmission of neurons, suggesting that the effects of radiation exposure appear at the presynaptic terminals. Furthermore, the frequency of mEPSC depends on the density change of the dendritic spines on the postsynaptic cell, and the signal intensity is considered to depend on the post-side change and/or the spine size[36]. It is reported that the spine form changes during conditions such as mental retardation and memory impairment, and changes in conjunction with learning ability, the ovulatory cycle, spine shape and spine number are correlated with the synaptic transmission efficiency[37-40]. It is also known that irradiation with X-rays and photons, which has a higher biological effect ratio in comparison to X-rays, affects the ability to acquire molecular biological memory[41,42]. Another previous study has also assessed the impact of ionizing irradiation on neuronal intrinsic properties and synaptic signaling. Radiation led to early decreases in tyrosine phosphorylation and removal of excitatory N-methyl-D-aspartate receptors from the cell surface while simultaneously increasing the surface expression of inhibitory gamma-aminobutyric acid receptors[43]. Dey *et al.* found that serotonin receptor levels were decreased in the hippocampus post-irradiation, and mice displayed both anxiety- and depression-like behaviors[44]. Newton *et al.* revealed by proteomic analysis the dysregulation of metabolic and signaling pathways, such as mitochondrial dysfunction, Rac 1 signaling, and synaptogenesis signaling, associated with neurocognitive dysfunction[45]. These alterations in cellular localization, receptor, or activity of signaling transduction corresponded with altered synaptic responses and inhibition of long-term potentiation. Furthermore, Shirai *et al.* demonstrated that X-ray irradiation decreases the dendritic spine density in a dose-dependent manner and changes the dendritic spine morphology thinner and longer than the non-irradiated spines by reducing the abundance of cytoskeletal proteins[2]. In addition, changes to the irradiated brain include depletion of stem cell populations accompanied by reductions in dendritic complexity and spine density, and radiation exposure initiates cyclical cascades of secondary reactive processes that involve oxidative stress and inflammation, which serve to perpetuate the signature of radiation injury over time[45,46]. In consideration of our result and the findings of various reports, although neurons have the ability to repair severe DNA damage, even when irradiated with high doses of X-rays, there is a high possibility that some change, such as density or morphology, has occurred in the dendritic spines which have essential functions in synaptic transmission.

The present study revealed that neuron has high resistance for irradiation but has an influence on the synaptic transmission. Our data showed that the frequency of mEPSCs was increased, at least in part by some morphological changes and molecular biological changes might occur in the dendritic spines. Radiotherapy has been widely used in the treatment of brain tumors; however, cognitive impairment due to radiation exposure has been drawing attention as the number of patients who achieve long-term survival after radiotherapy increases[47-49]. Only concomitant adverse events may be noticeable, especially if the tumor has low proliferative potential[50]. Therefore, it is very important to elucidate the mechanism underlying the occurrence of adverse events, estimate the degree of cognitive impairment, and promote efforts to improve the prognosis. Further studies should be undertaken to analyze the relationship between radiation exposure and the morphological changes of spines, as well as the mechanisms of the individual effects of whole brain irradiation, such as the effects on memory and behavior.

Acknowledgments

This work was supported by Hirosaki University Institutional Research Grant FY2014-2016.

Conflict of interests

The authors have no potential conflicts of interest to declare.

Author contributions

TN, YM and JY designed the study; MY, TT, TF, SS and JY performed the experiments; MY, TT, TN, YM and JY wrote this manuscript. All authors contributed extensively to discussions regarding the work and the review of the manuscript.

References

1. Mukai Y, Ueno H. Establishment and implementation of Cancer Genomic Medicine in Japan. Cancer Sci. 2021;112:970–7.
2. Shirai K, Mizui T, Suzuki Y, Okamoto M, Hanamura K, Yoshida Y, *et al.* X irradiation changes dendritic spine morphology and density through reduction of cytoskeletal proteins in mature neurons. Radiat Res. 2013;179:630–6.
3. Aoyama H, Shirato H, Tago M, Nakagawa K, Toyoda T, Hatano K, *et al.* Stereotactic radiosurgery plus whole-brain radiation therapy vs stereotactic radiosurgery alone for treatment of brain metastases: a randomized controlled trial. JAMA. 2006;295:2483–91.
4. Stupp R, Mason WP, den Bent MJ, Weller M, Fisher B, Taphoorn MJB, *et al.* Radiotherapy plus concomitant and adjuvant temozolomide for glioblastoma. N Engl J Med. 2005;352:987–96.

5. Sheline GE, Wara WM, Smith V. Therapeutic irradiation and brain injury. Int J Radiat Oncol Biol Phys. 1980;6:1215–28.
6. Dropcho EJ. Central nervous system injury by therapeutic irradiation. Neurol Clin. 1991;9:969–88.
7. Wefel JS, Kayl AE, Meyers CA. Neuropsychological dysfunction associated with cancer and cancer therapies: A conceptual review of an emerging target. Br J Cancer. 2004;90:1691–6.
8. Greene-Schloesser D, Robbins ME, Peiffer AM, Shaw EG, Wheeler KT, Chan MD. Radiation-induced brain injury: A review. Front Oncol. 2012;2:73.
9. Maldaun MVC, Aguiar PHP, Lang F, Suki D, Wildrick D, Sawaya R. Radiosurgery in the treatment of brain metastases: critical review regarding complications. Neurosurg Rev. 2008;31:1–9.
10. Marks JE, Baglan RJ, Prassad SC, Blank WF. Cerebral radionecrosis: incidence and risk in relation to dose, time, fractionation and volume. Int J Radiat Oncol Biol Phys. 1981;7:243–52.
11. Ruben JD, Dally M, Bailey M, Smith R, McLean CA, Fedele P. Cerebral radiation necrosis: incidence, outcome, and risk factors with emphasis on radiation parameters and chemotherapy. Int J Radiat Oncol Biol Phys. 2006;65:499–508.
12. Van Oosterhout AG, Ganzevles PG, Wilmink JT, De Geus BW, Van Vonderen RG, Twijnstra A. Sequelae in long-term survivors of small cell lung cancer. Int J Radiat Oncol Biol Phys. 1996;34:1037–44.
13. Ebi J, Sato H, Nakajima M, Shishido F. Incidence of leukoencephalopathy after whole-brain radiation therapy. Int J Radiat Oncol Biol Phys. 2013;85:1212–7.
14. Harila-Saari AH, Pääkkö EL, Vainionpää LK, Pyhtinen J, Lanning BM. A longitudinal magnetic resonance imaging study of the brain in survivors in childhood acute lymphoblastic leukemia. Cancer. 1998;83:2608–17.
15. Hertzberg H, Huk WJ, Ueberall MA, Langer T, Meier W, Dopfer R, *et al*. CNS late effects after ALL therapy in childhood. Part I: Neuroradiological findings in long-term survivors of childhood ALL–an evaluation of the interferences between morphology and neuropsychological performance. The German Late Effects Working Group. Med Pediatr Oncol. 1997;28:387–400.
16. Asai A, Matsutani M, Kohno T, Nakamura O, Tanaka H, Fujimaki T, *et al*. Subacute brain atrophy after radiation therapy for malignant brain tumor. Cancer. 1989;63:1962–74.
17. Shibamoto Y, Baba F, Oda K, Hayashi S, Kokubo M, Ishihara S, *et al*. Incidence of brain atrophy and decline in mini-mental state examination score after whole-brain radiotherapy in patients with brain metastases: a prospective study. Int J Radiat Oncol Biol Phys. 2008;72:1168–73.
18. Armstrong CL, Corn BW, Ruffer JE, Pruitt AA, Mollman JE, Phillips PC. Radiotherapeutic effects on brain function: double dissociation of memory systems. Neuropsychiatry Neuropsychol Behav Neurol. 2000;13:101–11.
19. Aoyama H, Tago M, Kato N, Toyoda T, Kenjyo M, Hirota S, *et al*. Neurocognitive function of patients with brain metastasis who received either whole brain radiotherapy plus stereotactic radiosurgery or radiosurgery alone. Int J Radiat Oncol Biol Phys. 2007;68:1388–95.
20. Soussain C, Ricard D, Fike JR, Mazeron JJ, Psimaras D, Delattre JY. CNS complications of radiotherapy and chemotherapy. Lancet. 2009;374:1639–51.
21. Chang EL, Wefel JS, Hess KR, Allen PK, Lang FF, Kornguth DG, *et al*. Neurocognition in patients with brain metastases treated with radiosurgery or radiosurgery plus whole-brain irradiation: a randomized controlled trial. Lancet Oncol. 2009;10:1037–44.
22. Armstrong CL, Shera DM, Lustig RA, Phillips PC. Phase measurement of cognitive impairment specific to radiotherapy. Int J Radiat Oncol Biol Phys. 2012;83:319–24.
23. Mariya Y, Saito F, Kimura T, Aoki M, Anbai A, Basaki K, *et al*. Cerebral function estimation using electro-encephalography for the patients with brain tumor managed by radiotherapy. Japanese Journal of Clinical Radiology. 1999;44:1163–70 (in Japanese with English abstract).
24. Fuchs E, Flugge G. Adult Neuroplasticity: More than 40 years of research. Neural Plast. 2014;2014:541870.
25. Hall EJ. Radiobiology for the radiologist. 3rd Edition. Philadelphia:Lippincott;1988. pp357–364.
26. Yamada J, Inoue K, Furukawa T, Fukuda A. Low-concentration tributyltin perturbs inhibitory synaptogenesis and induces neuronal death in immature but not mature neurons. Toxicol Lett. 2010;198:282–8.
27. Marková E, Torudd J, Belyaev I. Long time persistence of residual 53BP1/γ-H2AX foci in human lymphocytes in relationship to apoptosis, chromatin condensation and biological dosimetry. Int J Radiat Biol. 2011;87:736–45.
28. Ward JF. DNA damage produced by ionizing radiation in mammalian cells: identities, mechanisms of formation, and reparability. Prog Nucleic Acid Res Mol Biol. 1988;35:95–125.
29. Ueno T, Yamada J, Nishijima H, Arai A, Migita K, Baba M, *et al*. Morphological and electrophysiological changes in intratelencephalic-type pyramidal neurons in the motor cortex of a rat model of levodopa-induced dyskinesia. Neurobiol Dis. 2014;64:142–9.
30. Katz B, Miledi R. Tetrodotoxin-resistant electric activity in presynaptic terminals. J Physiol. 1969;203:459–87.
31. Inoue K, Yamada J, Ueno S, Fukuda A. Brain-type creatine kinase activates neuron-specific K+-Cl- co-transporter KCC2. J Neurochem. 2006;96:598–608.
32. Brown WR, Thore CR, Moody DM, Robbins ME, Wheeler KT. Vascular damage after fractionated whole-brain irradiation in rats. Radiat Res. 2005;164:662–8.
33. Fink J, Born D, Chamberlain MC. Radiation necrosis: relevance with respect to treatment of primary and secondary brain tumors. Curr Neurol Neurosci Rep. 2012;12:276–85.
34. Kim JH, Brown SL, Jenrow KA, Ryu S. Mechanisms of radiation-induced brain toxicity and implications for future clinical trials. J Neurooncol. 2008;87:279–86.
35. Siu A, Wind JJ, Iorgulescu JB, Chan TA, Yamada Y, Sherman JH. Radiation necrosis following treatment of high-grade glioma--a review of the literature and current understanding. Acta Neurochir (Wien). 2012;154:191–201.
36. Holtmaat A, Svoboda K. Experience-dependent structural synaptic plasticity in the mammalian brain. Nat Rev Neurosci. 2009;10:647–58.
37. Hanamura K, Shirao T. Actin cytoskeleton in dendritic spine. Folia Pharmacol. Jpn. 2007;130:352–7.
38. Woolley CS, Gould E, Frankfurt M, McEwen BS. Naturally occurring fluctuation in dendritic spine density on adult hippocampal pyramidal neurons. J Neurosci. 1990;10: 4035–9.
39. Moser MB, Trommald M, Andersen P. An increase in dendritic spine density on hippocampal CA1 pyramidal cells following spatial learning in adult rats suggests the formation of new synapses. Proc Natl Acad Sci USA. 1994;91:12673–5.
40. Matsuzaki M, Ellis-Davies GC, Nemoto T, Miyashita Y, Iino M, Kasai H. Dendritic spine geometry is critical for AMPA receptor expression in hippocampal CA1 pyramidal neurons. Nat Neurosci. 2001;4:1086–92.
41. Parihar VK, Pasha J, Tran KK, Craver BM, Acharya MM, Limoli CL. Persistent changes in neuronal structure and synaptic

plasticity caused by proton irradiation. Brain Struct Funct. 2015;220:1161–71.

42. Puspitasari A, Koganezawa N, Ishizuka Y, Kojima N, Tanaka N, Nakano T, *et al*. X irradiation induces acute cognitive decline via transient synaptic dysfunction. Radiat Res. 2016;185:423–30.

43. Wu PH, Coultrap S, Pinnix C, Davies KD, Tailor R, Ang KK, *et al*. Radiation induces acute alterations in neuronal function. PLoS One. 2012;7:e37677.

44. Dey D, Parihar VK, Szabo GG, Klein PM, Tran J, Moayyad J, *et al*. Neurological impairments in mice subjected to irradiation and chemotherapy. Radiat Res. 2020;193:407–24.

45. Newton J, Brown T, Corley C, Alexander T, Trujillo M, McElroy T, *et al*. Cranial irradiation impairs juvenile social memory and modulates hippocampal physiology. Brain Res. 2020;1748:147095.

46. Hinzman CP, Baulch JE, Mehta KY, Gill K, Limoli CL, Cheemaa AK. Exposure to ionizing radiation causes endoplasmic reticulum stress in the mouse hippocampus. Radiat Res. 2018;190:483–93.

47. Noguchi J, Matsuzaki M, Ellis-Davies GC, Kasai H. Spine-neck geometry determines NMDA receptor-dependent Ca2+ signaling in dendrites. Neuron. 2005;46:609–22.

48. Crossen JR, Garwood D, Glatstein E, Neuwelt EA. Neurobehavioral sequelae of cranial irradiation in adults: a review of radiation-induced encephalopathy. J Clin Oncol. 1994;12:627–42.

49. Roman DD, Sperduto PW. Neuropsychological effects of cranial radiation: current knowledge and future directions. Int J Radiat Oncol Biol Phys. 1995;31:983–98.

50. Iwadate Y, Fukuda K, Matsutani T, Saeki N. Adverse effects of radiation therapy in treating Gliomas. Jpn J Neurosurg. 2014;23:569–80.